

Dengue virus type 2 replication is limited by activation of NOD2 and its interactions with RIP2 and MAVS adaptors in THP-1 macrophage-like cells

Diana Domínguez-Martínez¹, Daniel Nuñez Avellaneda², Juan Castillo Cruz³, Gloria León-Avila⁴, BLANCA GARCIA-PEREZ⁵, and Ma. Isabel Salazar⁶

¹Hospital Infantil de Mexico Federico Gomez

²Iowa State University

³Instituto Politecnico Nacional

⁴Instituto Politécnico Nacional

⁵INSTITUTO POLITECNICO NACIONAL

⁶Escuela Nacional de Ciencias Biologicas

April 19, 2021

Abstract

The nucleotide-binding domain (NBD) and leucine-rich repeat receptors, such as NOD-like receptors (NLRs), have pivotal functions in the innate immune response to various viral infections participating during the recognition of pathogens and activation of signaling pathways. One NLR, NOD2, is a dynamic protein that is activated in the presence of viral genomes and metabolites. However, its participation in combating a dengue virus (DENV) infection remains unclear. The aim of this study was to determine the role of NOD2 in macrophage-like THP-1 cells during an *in vitro* infection with DENV type 2 (DENV2). The interactions of NOD2 with RIP2 and MAVS was examined in DENV2-infected and agonist-stimulated cells. The effects of downregulating NOD2 expression or signaling on virus loads was also evaluated. The cellular mRNA expression and protein levels of NOD2 on cells under the stimuli were quantified with RT-PCR, Western blot and indirect immunofluorescence. Both the mRNA and protein expression of NOD2 was enhanced in response to DENV-2 infection. Interactions of NOD2 with RIP2 and MAVS, analyzed with confocal microscopy and co-immunoprecipitation assays, were time-dependent and increased in the post-infection period, between 6 and 24 h. After silencing NOD2 expression, DENV2-infected cells displayed greater viral loads and decreased expression of IL-8 and IFN- α (measured in supernatants obtained from the cells), compared to the uninfected (mock control) cells or those transfected with irrelevant-siRNA. Thus, in response to a DENV2 infection, NOD2 was activated in THP-1 human macrophage-like cells, the production of IL-8 and IFN- α was enhanced, and viral replication was limited.

Dengue virus type 2 replication is limited by activation of NOD2 and its interactions with RIP2 and MAVS adaptors in THP-1 macrophage-like cells

Diana Alhelí Domínguez-Martínez^{1,2}, Daniel Núñez-Avellaneda^{1,3,4}, Juan Castillo-Cruz⁵, Gloria León-Avila⁶, Blanca Estela García-Pérez⁵ and Ma. Isabel Salazar^{1,3*}

1. Laboratorio de Inmunología Celular e Inmunopatogénesis, Departamento de Inmunología. Escuela Nacional de Ciencias Biológicas. Instituto Politécnico Nacional. CDMX, México.
2. Unidad de Investigación en Virus y Cáncer. Hospital Infantil de México “Federico Gómez”. CDMX, México.
3. Laboratorio de Virología e Inmunovirología, Departamento de Microbiología. Escuela Nacional de Ciencias Biológicas Instituto Politécnico Nacional. CDMX, México.

4. Department of Veterinary Microbiology and Preventive Medicine, College of Veterinary Medicine, Iowa State University, Ames, Iowa.
5. Laboratorio de Microbiología General, Departamento de Microbiología. Escuela Nacional de Ciencias Biológicas, Instituto Politécnico Nacional. CDMX, México.
6. Laboratorio de Genética, Departamento de Zoología, Escuela Nacional de Ciencias Biológicas, Instituto Politécnico Nacional. CDMX, México.

* Correspondence: isalazarsan@yahoo.com. Tel.: +52 (55) 5729-6000 Ext. 62576. Fax: +52 (55) 5729-6000 Ext. 43211.

Abstract

The nucleotide-binding domain (NBD) and leucine-rich repeat receptors, such as NOD-like receptors (NLRs), have pivotal functions in the innate immune response to various viral infections participating during the recognition of pathogens and activation of signaling pathways. One NLR, NOD2, is a dynamic protein that is activated in the presence of viral genomes and metabolites. However, its participation in combating a dengue virus (DENV) infection remains unclear. The aim of this study was to determine the role of NOD2 in macrophage-like THP-1 cells during an *in vitro* infection with DENV type 2 (DENV2). The interactions of NOD2 with RIP2 and MAVS was examined in DENV2-infected and agonist-stimulated cells. The effects of downregulating NOD2 expression or signaling on virus loads was also evaluated. The cellular mRNA expression and protein levels of NOD2 on cells under the stimuli were quantified with RT-PCR, Western blot and indirect immunofluorescence. Both the mRNA and protein expression of NOD2 was enhanced in response to DENV-2 infection. Interactions of NOD2 with RIP2 and MAVS, analyzed with confocal microscopy and co-immunoprecipitation assays, were time-dependent and increased in the post-infection period, between 6 and 24 h. After silencing NOD2 expression, DENV2-infected cells displayed greater viral loads and decreased expression of IL-8 and IFN- α (measured in supernatants obtained from the cells), compared to the uninfected (mock control) cells or those transfected with irrelevant-siRNA. Thus, in response to a DENV2 infection, NOD2 was activated in THP-1 human macrophage-like cells, the production of IL-8 and IFN- α was enhanced, and viral replication was limited.

Keywords: DENV, NOD2, RIP2, MAVS, IFN, macrophages

Introduction

Dengue is one of the most challenging arthropod-borne viral diseases in humans, causing around 390 million annual cases worldwide [1]. According to the WHO, dengue is a leading cause of serious disease and mortality, mostly in Latin America and Asia. It has four antigenically related serotypes (DENV-1, DENV-2, DENV-3, and DENV-4) and various genotypes within each one [2]. DENV belongs to the *Flaviviridae* family, which has viral particles approximately 50 nm in diameter with icosahedral capsids wrapped in a lipid bilayer envelope. This family has single-stranded RNA (ssRNA) genomes of positive polarity (~10.8 Kb long), with a single open reading frame encoding a single polyprotein. The latter is proteolytically processed by both viral and cellular proteases to produce three structural proteins (C, prM and E) and seven non-structural proteins (NS1, NS2A, NSB, NS3, NS4A, NS4B and NS5) [3].

Although the human cells targeted by DENV are predominantly monocytes, they also include macrophages, immature dendritic cells, mature dendritic cells, and reactive splenic lymphoid cells [4-7]. In such cells, DENV triggers the innate immune response (the first line of defense against infection), activating several pattern recognition receptors (PRRs) that mediate the rapid production of type I interferon (IFN α/β) and cytokines. Hundreds of interferon-stimulated genes (ISGs, induced by interferon IFN), modulate other branches of the immune response [8]. The orchestration of these effectors is capable of creating an antiviral state in both uninfected and infected cells through a variety of mechanisms [9].

PRRs are receptors of innate immune cells responsible for recognizing specific components (patterns) in pathogens. For viral components, ssRNA is recognized by TLR7 [10], double-stranded RNA (dsRNA, formed during viral replication) by RIG-I and MDA-5 molecules [11,12], and the glycoprotein of the viral envelope

by TLR3 [13,14]. During the infection of Huh-7 cells, DENV is recognized by two types of PRRs that act synergistically to restrict viral replication by triggering type I IFNs [12,14]. These two types of PRRs are membrane-bound TLR3 and cytoplasmic RLRs, the latter being RIG-I-like receptors (e.g., RIG-I and MDA-5).

In DENV2-infected M1 macrophages (known to exhibit an inflammatory phenotype), the NLRP3 inflammasome (a member of the NOD-like receptor (NLR) family) processes caspase-1, leading to the production of the active forms of IL-1 β and IL-18 and the generation of pyroptosis [15]. In platelets exposed to DENV, moreover, the NLRP3 inflammasome is activated to modulate the release of IL-1 β in micro-particles through mechanisms possibly dependent on mitochondrial activity [16]. However, the role of other intracellular PRRs (e.g., some NLRs) in DENV infections has not been clearly defined.

NOD2, a member of the NLR family, was initially described as a cytosolic sensor for muramyl dipeptide (MDP) [17]. The activation of NOD2 has been established in the presence of genomes and metabolites from viruses, triggering and modulating diverse immune signaling pathways related to nuclear factor kappa B (NF- κ B), IFN regulatory factor (IRF) 3/7, mitogen-activated protein kinase (MAPK) and others [18]. NOD2 is activated when interacting with proteins involved in enhancing antiviral signaling pathways, such as mitochondrial antiviral signaling protein (MAVS) [19], receptor-interacting serine/threonine-protein kinase 2 (RIP2) [20,21] and 2'-5'-oligoadenylate synthetase 2 (OAS2) [22]. Even though NOD2 has been implicated in a response to compounds that decrease cytokine production and viral replication in cultured human monocytes infected by dengue, its specific role during DENV infection has not yet been determined [23].

RIP2 has been reported to modulate the apoptotic pathway, mainly at 48 h post-infection (hpi), in HepG2 cells infected with DENV2 at a multiplicity of infection (MOI) of 1 [24]. Nevertheless, the specific involvement of RIP2 during a DENV2 infection in monocytes, macrophages and other types of cells is still unclear. In contrast, the participation of MAVS in activating the antiviral responses of type I IFNs is well known. Its activation occurs when RIG-1 (a cytosolic protein) detects DENV [25]. There are descriptions in the literature of anti-DENV activities mediated by members of the OAS family, including OAS1 p42, OAS1 p46 and OAS3 p100. Various human OAS proteins appear to be differentially induced in distinct types of cells and are characterized by different subcellular locations and enzymatic parameters [26]. A recent study revealed increased levels of mRNA of OAS1, OAS2 and OAS3 in U-937 macrophage-like cells infected with DENV2 [27].

The aim of the current study was to determine the role of NOD2 in macrophage-like THP-1 cells during an *in vitro* DENV2 infection. The interactions of NOD2 with effector molecules (RIP2 and MAVS) was examined in DENV2-infected and agonist-stimulated cells. The effects of downregulating NOD2 expression or signaling was also evaluated. The overall effect on viral replication was assessed.

Materials and Methods

DENV2 strains, culture and titration

The dengue virus employed presently is the Yuc17438 strain of serotype 2, which was isolated from a patient in Yucatán, Mexico. DENV2 was cultivated on C6/36 confluent monolayers obtained from the American Type Culture Collection (ATCC, Manassas, VA, USA), and cultured in Leibovitz's L-15 medium (Sigma-Aldrich, St. Louis, MO, USA) supplemented with L-glutamine, MEM non-essential amino acids solution, MEM vitamin solution, penicillin-streptomycin, 10 % of fetal bovine serum (FBS), and sodium pyruvate solution (all from Gibco, Waltham, MA, USA). Infections were carried out in Leibovitz's L-15 medium with 2% FBS. A mock uninfected control was treated under the same conditions. After 7 days, the supernatant of both virus-infected and uninfected (mock control) C6/36 cells was harvested by centrifugation at 2,000 g for 10 min. Subsequently, both supernatants were diluted to a final concentration of 8% in polyethylene glycol 8000 (Sigma-Aldrich) solution with PBS 1x (Gibco) and incubated overnight at 4 °C. The next day each solution was centrifuged at 6,000 g for 1 h. The pellets were re-suspended at 1/10 of the total solution volume in L-15 medium supplemented with 10% FBS, then aliquoted and frozen at -70°C until needed.

Viral stocks and supernatant from the mock group were titrated in focus forming assays on C6/36 cells. Briefly, 10-fold serial dilutions of viral stock (200 μ L) were used to infect cells on monolayers in 24-well plates. After 1 h of gentle agitation, each well (containing C6/36 cells supplemented with 2% of FBS) was covered with 1 mL of overlay medium consisting of 1% carboxymethyl cellulose (Sigma-Aldrich) in L-15 medium. The overlay medium was gently removed 5 days later, and monolayers were fixed with 30% acetone in cold PBS 1x for 20 min at 4 °C. The foci in C6/36 cells were then stained with a primary anti-DENV-envelope antibody (clone 4G2) (Merck-Millipore, Burlington, MA, USA) coupled to a secondary antibody and anti-mouse IgG-HRP (Invitrogen, Carlsbad, CA, USA). Finally, the foci were revealed with the substrate 3,3'-diaminobenzidine (DAB) (Diagnostic Biosystems Inc., Pleasanton, CA, USA). Viral titers were expressed as focus forming units (FFU)/mL or plaque forming units (PFU)/mL. The experiments were performed with an MOI of 10.

THP-1 cell culture and macrophage differentiation

The THP-1 (human monocytic leukemia) cell line was acquired from ATCC and cultured in RPMI-1640 medium (Gibco) supplemented with sodium pyruvate solution, L-glutamine, penicillin-streptomycin, MEM non-essential amino acids solution, and 10% FBS (all from Gibco). The macrophage-like state was optimally obtained by treating THP-1 cells for 3 days with 100 ng/mL of phorbol 12-myristate 13-acetate (PMA, Sigma-Aldrich) under several experimental conditions. Subsequently, adherent cells (THP-1 macrophage-like cells) were gently washed three times with PBS 1x (Gibco) and left to stand with fresh RPMI-1640 medium for 5 days before further use.

L18-MDP or PIC transfections

THP-1 macrophage-like cells were transfected with a mixture of LipofectamineTM 3000 reagent (LP3000) (Invitrogen, Carlsbad, CA, USA) and L18-MDP (2 μ g/mL) (Invivogen, San Diego, CA, USA) or PIC (2 μ g/mL) (Sigma-Aldrich), prepared according to the manufacturer's instructions. The cells were then incubated at room temperature for 5 min. Afterwards, each mixture was placed on the monolayer to reach a final volume of 1 mL of Opti-MEM medium (Gibco) and were incubated at 37 °C in 5% CO₂ for the indicated periods of time.

Confocal microscopy

THP-1 cells (3x10⁵ cells/mL) were seeded on glass cover slips in a 24-well tissue culture plate (Corning, NY, USA). Upon completion of the differentiation protocol, cells were either infected with DENV2, transfected with L18-MDP or PIC (described above), or left untreated (mock control). Briefly, the viral stocks were adjusted to an MOI of 10 in a supplemented RPMI medium and incubated at 37 °C for 1 h on monolayers, after which time the cells were washed three times with PBS 1x (Gibco) and fixed with 2% of paraformaldehyde (Sigma) for 15 min at rt. Subsequently, the cells were permeabilized with 0.1% Triton X-100 (Sigma-Aldrich) in 1 x PBS for 15 min and blocked with 5% bovine serum albumin (BSA, Sigma-Aldrich) at room temperature for 1 h. Upon completion of this time, addition was made of the primary antibodies: anti-NS3, anti-NOD2, anti-RIP2, anti-MAVS (Genetex Inc., Irvine, CA, USA) and in each case incubation was carried out at room temperature for 2 h. The cells were then washed three times with PBS 1x before the secondary antibodies were added. An anti-mouse IgG coupled to the DyLight-488 antibody (Pierce Biotechnology Inc., Waltham, MA, USA) was utilized for NOD2, and an anti-rabbit IgG coupled to the APC antibody (Santa Cruz Biotechnology Inc., Santa Cruz, CA, USA) for NS3, RIP2 and MAVS. All were incubated at room temperature for 30 min in the dark. Finally, the nuclei were labeled with DAPI (Sigma-Aldrich) for 15 min and the slides were mounted with Vectashield (Vector Laboratories, Burlingame, CA, USA). The images of 100 cells per condition were captured on a confocal laser scanning system (LSM5 Pascal) attached to a confocal microscope (Axiovert 200 M, Zeiss, Jena, Germany). For colocalization analysis in confocal microscopy, JACoP program of Image J software was used for different captured fields accounting in total for N=100 cells for each different experimental condition, then an overlap coefficient was obtained. Cell culture supernatants from those cells were collected and frozen at -70°C to await cytokine measurement or viral titration.

mRNA analysis

Total cellular RNA was isolated with TRIzol (Invitrogen) as specified in the manufacturer's instructions. For reverse transcription (RT), the RNA was quantified in a NanodropTM from Thermo Sc. (Rockford, IL, USA) and then 1 μ g of total RNA were added with 0.5 μ g of oligo-dT (Thermo Sc.) and incubated at 70 °C for 10 min. The RT reaction included 1 \times single strand buffer, 500 mM of each deoxynucleotide triphosphate (Roche, Mannheim, Germany), and RevertAid reverse transcriptase (200 U) (Thermo Sc). Each RT reaction was incubated at 42 °C for 1 h to furnish cDNA. On each cDNA strand obtained, PCR was performed in a commercial master mix with 2.0 mM MgCl₂ (Amplicon III, Odense M, Denmark). The human GAPDH gene served as the endogenous control. The following primers sequences (Invitrogen) were used for RT-PCR: GAPDH, forward 5'-GGTCATCCATGACAACCTTTGG-3' and reverse 5'-GTCATACCAGGAAATGAGCTTGAC-3'; NOD2, forward 5'-CAGCTGGACTACAACCTCTGTGG-3' and reverse 5'-GCAGAGTTCTTCTAGCATGACG-3'. All readings were normalized to the mRNA level of GAPDH.

Western blot

For Western blot analysis, THP-1 macrophage-like cells differentiated in 6-well plates (2 \times 10⁶ cells/well) were separated into groups: infected with DENV2, transfected with L18-MDP or PIC, and untreated (mock control). Upon completion of the time of each treatment, cells were lysed with RIPA buffer (50 mM Tris HCl, pH 8, 150 mM NaCl, 1% NP-40, 0.5% sodium deoxycholic acid and 0.1% SDS), which contains a protease inhibitor cocktail (COMpleteTM, Roche Diagnostic GmbH, Mannheim, Germany). The total protein concentration was determined by employing a PierceTM BCA protein assay kit (Thermo Fisher Scientific, Rockford, IL, USA) according to the manufacturer's instructions. Forty μ g of total protein were separated by 10% SDS-PAGE and transferred to a nitrocellulose membrane (Bio-Rad Laboratories, Berkeley, CA, USA). Membranes were blocked with 5% non-fat milk in PBS 1x for 1 h and then membranes were immunostained as described elsewhere. Proteins were visualized with Luminata Forte substrate (Merck-Millipore) and the immunoreactive proteins were detected by exposure to Kodak Carestream film (Sigma-Aldrich).

Co-immunoprecipitation assays

For these assays, THP-1 macrophage-like cells were differentiated in a T-25 cell culture flask (5 \times 10⁶ cells/flask). Subsequently, they were infected with DENV2, transfected with L18-MDP or PIC, and untreated (mock control). When the incubation period of each treatment was completed, cells were lysed with RIPA buffer containing a cocktail protease inhibitor (previously mentioned). Total protein lysates were quantified as previous detailed, and 150 μ g of total protein were incubated with an anti-NOD2 antibody (2 μ g/reaction) overnight at 4°C with constant rocking. Subsequently, 15 μ L of protein A agarose beads (Thermo Sc.) were added to each mixture and incubated while gently mixing by constantly inverting the tube at 4 °C for 3 h. The precipitates were then washed eight times with PBS 1x-protease inhibitors, the pellets were re-suspended, and the NOD2-RIP2 and NOD2-MAVS interactions were evaluated with an immunoblot assay. Immunoblots were probed with the following antibodies: anti-RIP2 and anti-MAVS (previously explained) coupled to an anti-rabbit IgG-HRP conjugated antibody. They were visualized by using enhanced chemiluminescence with Luminata Forte substrate (Merck-Millipore).

Small interfering RNA (siRNA) assays

A total of 2.5 \times 10⁶ THP-1 macrophage-like cells in 6-well plates were transfected with a mixture of two siRNAs Card4 (25 pmol) and Card6 (25 pmol) against human NOD2 (NOD2-siRNAs, catalog number 1027415, Qiagen, Hilden, Germany). As a negative control, AllStars negative control siRNA (irrelevant-siRNA 50 pmol, catalog number 1027281, Qiagen) were transfected with LP3000 (Invitrogen), as specified in the manufacturer's protocol, for 12 h. Cell viability was determined with the MTT assay (Sigma-Aldrich). Briefly, 15 μ g of MTT reagent (500 μ g/mL) were added to each well and incubated at 37 °C for 3 h. Cells were then lysed with 100 μ L of DMSO (Sigma-Aldrich) and rocked until the purple formazan crystal was completely solubilized. Absorbance was measured at 600 nm in a microplate reader (Thermo Sc) and the percentage of cell viability was calculated with the resulting values, as follows: $(A_{\text{treatment}} - A_{\text{blank}})/(A_{\text{control}} - A_{\text{blank}}) \times 100\%$. Additionally, the efficiency of cells with NOD2 knocked down was assessed by Western

blot and indirect immunofluorescence, as described elsewhere.

Curcumin treatments

THP-1 macrophage-like cells (3×10^5 cells/mL) were seeded on 24-well tissue culture plates. After the differentiation protocol, cells were washed twice with PBS 1x. Curcumin (Sigma Aldrich) was diluted in ethanol according to manufacturer's instructions, adding $30 \mu\text{M}/\text{mL}$ [28] to each well for the treated group. Ethanol was added to control wells. Finally, the plates were incubated at 37°C for 1 h, and each stimulus was co-incubated as indicated elsewhere.

Determination of cytokine levels

The cytokine concentration was quantified in THP-1 cell culture supernatants. Distinct ELISA kits were employed for human IL-8 (Peprotech, Cranbury, NJ, USA) and human IFN- α (eBioscience, San Diego, CA, USA). Both measurements were performed as specified in the manufacturer's instructions.

Statistical Analysis

Differences between groups were analyzed on GraphPrism[®] version 8.0 (GraphPad Software Inc., San Diego, CA, USA). For comparison between three groups, significance was examined with one-way ANOVA. Comparisons between two groups of continuous variables were made with the Student's *t*-test in the case of parametric distributions and the Mann-Whitney U test for nonparametric distributions.

Results

DENV2 infection upregulates NOD2 expression

NOD2 expression was evaluated by confocal microscopy at distinct time points in THP-1 macrophage-like cells infected by DENV, transfected with L18-MDP, or untreated (mock control). There was a low expression of this molecule in the uninfected cells (Fig. 1A). A singular pattern of distribution was observed in the DENV2-infected cells from 6-24 hpi, with NOD2 localized in the cytosol in a characteristic pattern in approximately 15-20% of the cells (Fig. 1B). In contrast, ~40-50% of the cells transfected with synthetic L18-MDP (the positive control) exhibited a more vesicle-like pattern of distribution for NOD2 (Fig. 1C).

Macrophages derived from the THP-1 cell line are reported to be permissive for DENV2 infection *in vitro* [29]. As a control for DENV infection, the expression of viral NS3 protein (red) was examined, being detected at 12 hpi. The NS3 and NOD2 sites were found co-localized in 18% of double positive cells (Suppl. Fig. 1). On the other hand, the quantification of NOD2 mRNA in untreated (control) and DENV2-infected THP-1 macrophage-like cells showed the following increases in expression for the latter: 1.5-fold at 3 hpi, 2.6-fold at 6 hpi and 3.5-fold at 12 hpi. Treatment with L18-MDP resulted in the greatest increase in the expression of NOD2 of the three groups: 1.6-fold at 3 h, 4.3-fold at 6 h and 5.5-fold at 12 h (Fig. 1D). Western blot analysis confirmed the higher level of NOD2 in DENV2-infected and L18-MDP-transfected cells (compared to the control): 1.46-fold at 12 hpi and 3.1-fold at 24 hpi in the infected cells; 1.4-fold at 3 h, 2.45-fold at 6 h and 5-fold at 12 h in the transfected cells (Fig. 1E).

Figure 1

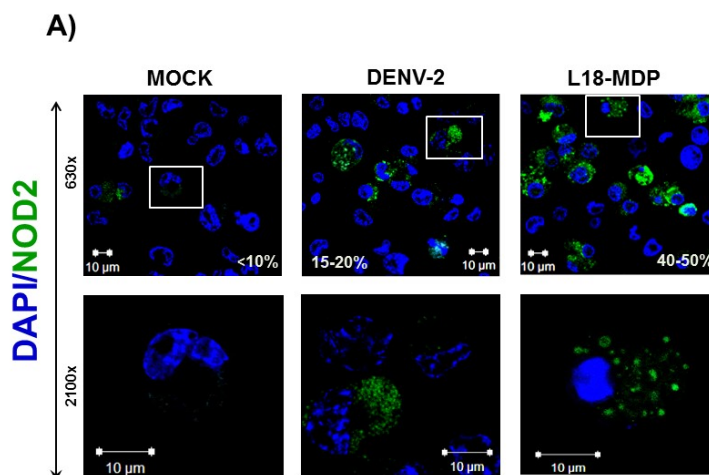


Figure 1

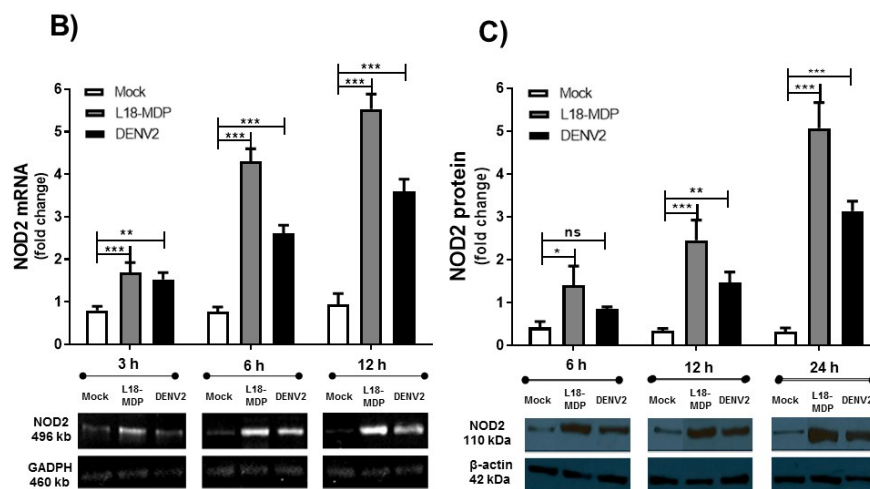


Figure 1. NOD2 was up-regulated in DENV2-infected and L18-MDP-transfected THP-1 cells. (A) Confocal micrograph of THP-1 macrophage-like cells having undergone the following treatments for 12 h: infection with DENV2, transfection with L18-MDP, or untreated (mock control). The cells were prepared by immunostaining for NOD2 (*green*) and nuclear contrast (*blue*). The micrograph (on the right) illustrates the entire field of each treatment, and a cell positive for NOD2 is depicted in the box. Images in the upper panels denote the percentage of NOD2 positive cells for each condition (N=110). The pictures (magnification 2100x) were cropped to improve the presentation. The bar graphs (B and C) portray the NOD2 expression

in cells at distinct time points post-infection under different treatments: Mock (white bars), transfected with L18-MDP (gray bars), or infected with DENV2 at an MOI of 10 (black bars). The bar graphs indicate the degree of increase (fold change) calculated by the ratio of NOD2/GAPDH (D) and NOD2/ β -actin (E). (B) mRNA of NOD2 was measured at 3, 6 and 12 h post-infection, using end point RT-PCR with specific primers for human NOD2 and GAPDH. (C) Relative NOD2 protein expression was established by Western blot analysis of the whole-cell lysates with an anti-NOD2 antibody. An anti- β -actin antibody served as the loading control. Representative gel and membrane images from RT-PCR and western blot at different time points are shown. Significance was determined with one-way ANOVA: *** $p < 0.001$, ** $p < 0.05$, * $p < 0.05$, and ns: not significant.

Expression of RIP2 and MAVS effectors and co-localization with NOD2

RIP2 was constitutively expressed in all experimental groups, including the untreated cells (Fig. 2A). Its expression was more abundant than that of NOD2 (Fig. 2D). At 6 hpi, DENV2-infected cells and L18-MDP-transfected cells both displayed an enhanced RIP2 expression (Figs. 2B and C). At this time point, co-localization of NOD2 and RIP2 was found in ~25% of the DENV2-infected cells (Fig. 2H), while co-localization was limited or absent in the mock-infected or transfected cells (Figs. 2G and I). At 12 hpi, the expression of the MAVS effector was absent in untreated cells (Fig. 3A), marginal in DENV2-infected cells (Fig. 3B), and slightly higher (than the infected group) in PIC-transfected cells. At the same time point, the increased expression of MAVS in the transfected cells correlated with the expression of NOD2 in the cytosol (Figs. 3C, F and I), and some co-localization between MAVS and NOD2 was observed in the DENV2-infected cells (Fig. 3H). A quantitative measure of cells showing some overlapping was carried out to have a more objective value using different microscopy fields as indicated in Suppl. Fig. 2.

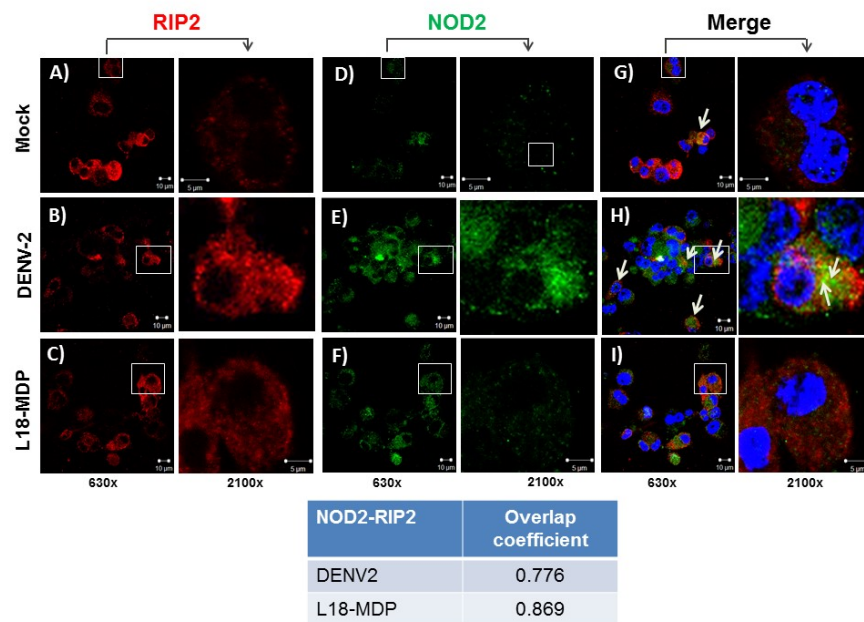


Figure 2. DENV2-induced NOD2-RIP2 co-localization is demonstrated in THP-1 macrophage-like cells. (A-C) Untreated (UT), DENV2-infected and L18-MDP-transfected cells are illustrated at 6 hpi. To evaluate NOD2-RIP2 co-localization, the cells were fixed, permeabilized and immunostained with an anti-RIP2 antibody (in red, D-F) and an anti-NOD2 antibody (in green, G-I). To the far right, the images of RIP2 (red) and NOD2 (green) are merged, with a nuclear contrast (blue). Individual cells portrayed in the square were selected for examination in greater detail. A digital magnification of 630x is shown on the left

and of 2100x on the right side of each column. Each condition was repeated three times. Overlap coefficient provided by JACoP program is shown for DENV treated (0.776) and L18-MDP positive control (0.869) after analyzing different fields.

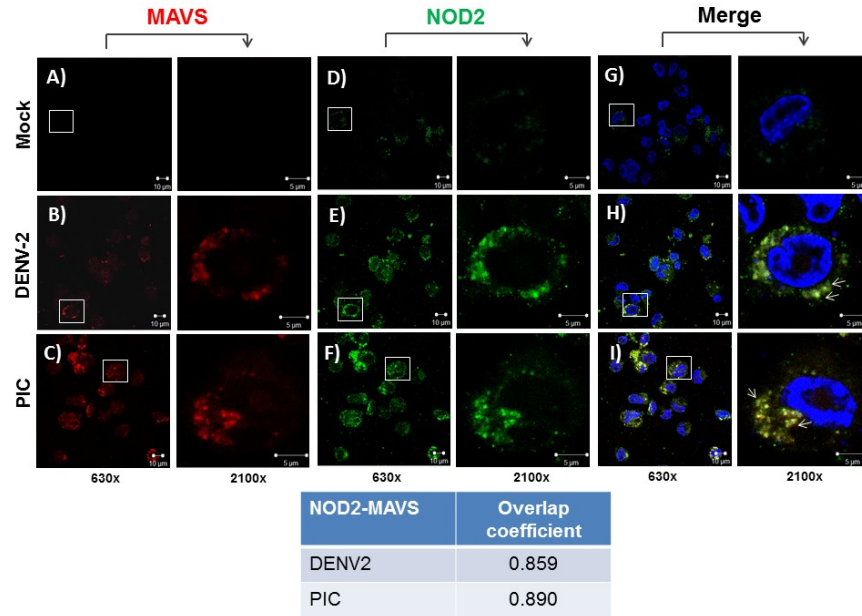


Figure 3. DENV2-induced NOD2-MAVS co-localization in THP-1 macrophage-like cells. (A-C) Untreated (UT), DENV2-infected and PIC-transfected cells can be appreciated at 12 hpi. To evaluate NOD2-MAVS co-localization, the cells were fixed, permeabilized and immunostained with an anti-MAVS antibody (in red, **D-F**) and an anti-NOD2 antibody (in green, **G-I**) . To the far right, the images of MAVS (red) and NOD2 (green) are merged, with a nuclear contrast (blue). Individual cells displayed in the square were selected for observation in greater detail. A digital magnification of 630x is illustrated on the left and 2100x on the right side of each column. Each condition was repeated three times. Overlap coefficient provided by JACoP program is shown for DENV treated (0.859) and L18-MDP positive control (0.890) after analyzing different fields.

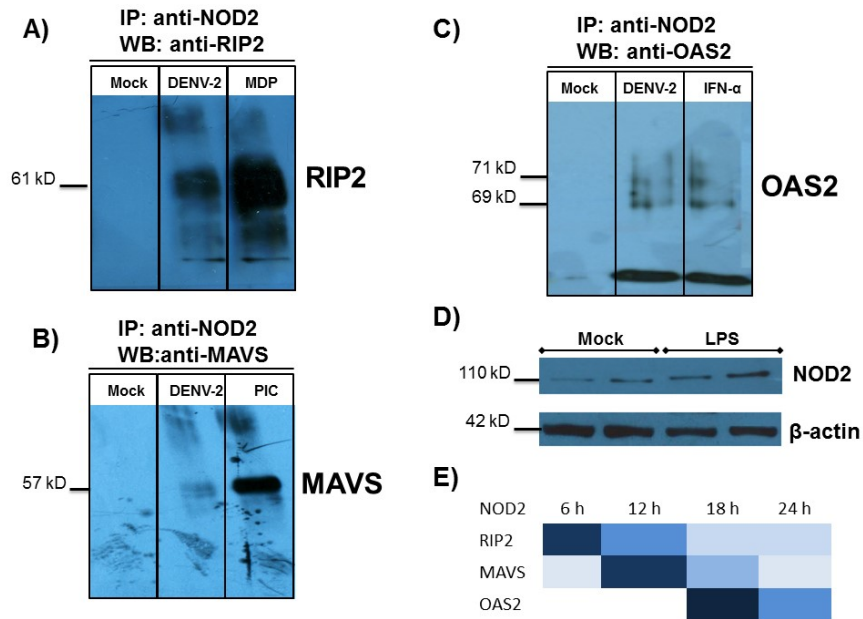


Figure 4. DENV2 induced NOD2-RIP2 and NOD2-MAVS protein interactions in THP-1 macrophage-like cells. The interaction of NOD2 with RIP2 and MAVS was measured by co-immunoprecipitation assays in whole protein cell lysates of the cells, which were mock treated, DENV2-infected, or given the corresponding treatment for the positive, immunoprecipitating in each case with anti-NOD2 antibody and immunoblotting with the indicated antibody. **(A)** Transfection with L18-MDP in positive control and the NOD2-RIP2 interaction evaluated 6 h later; and **(B)** transfected with PIC for positive control and the NOD2-MAVS interaction at 12 h. Subsequently, cells were harvested and lysed, and the total protein was quantified, also Western blot analysis of NOD2 in whole cell lysates alone was carried out in mock treated THP-1 cells and LPS (100 ng/mL) treated cells after 6 h **(C)**. Each interaction was analyzed by the co-immunoprecipitation of each molecule (by adding an anti-NOD2 antibody) followed by Western blotting. The immunoblots were performed by using specific antibodies for each molecule evaluated (RIP2 and MAVS), with each primary antibody being coupled to an anti-rabbit IgG-HRP secondary antibody. **(D)** Time-dependent interactions of NOD2 with RIP2 and MAVS found in the cells infected with DENV2 and interpreted in a colored map. Interaction rates are coded in shades of blue: dark blue indicates a higher interaction rate and light blue a lower interaction rate. Interaction rates were determined by co-immunoprecipitation assays and Western blot (as described in the text) at 6, 12, 18 and 24 h post-treatment (the measurement time post-infection is shown for each interaction). Each assay was repeated three times.

DENV2 infection induced the interaction of NOD2 with the effector proteins RIP2 and MAVS

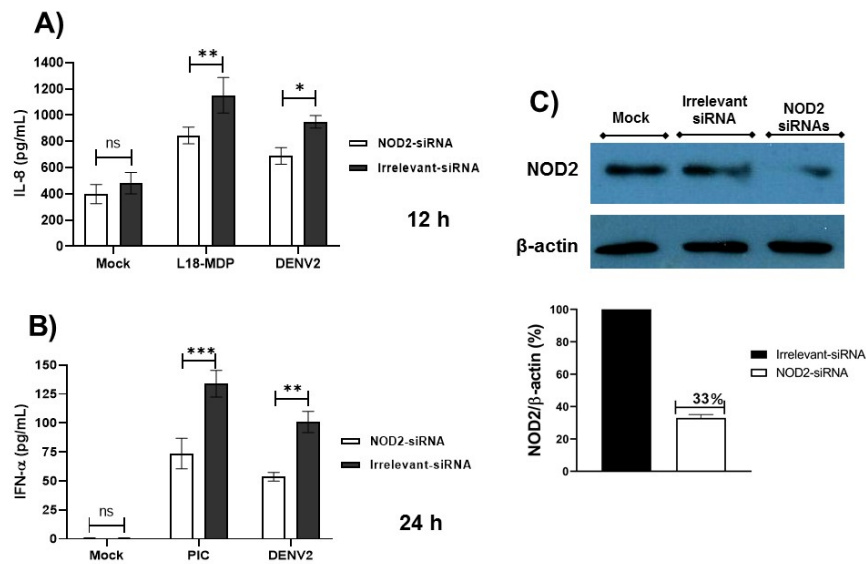
The protein interactions of RIP2 and MAVS proteins with NOD2 were revealed by co-immunoprecipitation assays in the three experimental groups of THP-1 macrophage-like cells (Figs. 4A-B). The interaction of NOD2 with RIP2 was assessed in lysates of the cells. The interaction was manifested in DENV2-infected and L18-MDP-transfected cells, but not in untreated cells (Fig. 4A). Likewise, the MAVS protein was recovered by co-immunoprecipitation in lysates of DENV2-infected and PIC-transfected cells at 12 hpi, but not in untreated cells (Fig. 4B). A general overview is portrayed of the NOD2-RIP2 and NOD2-MAVS interactions over time (Fig. 4E). A time-dependent interaction pattern emerged from the analysis, with the NOD2-RIP2 interaction appearing first at 6 hpi and the NOD2-MAVS interaction later at 12 hpi.

Downregulation of NOD2 in DENV2-infected cells increased viral replication and reduced production of IL-8 and IFN- α

The effects of NOD2 downregulation were examined with two approaches: gene silencing with siRNAs and chemical inhibition using curcumin. To assure the viability of cells subjected to a double round of transfections with siRNAs and agonists, proper assays were carried out. The corresponding assays demonstrated a high percentage of viability (80-88%) in cells treated with curcumin as well as the ones exposed to double transfections (Suppl. Fig. 3). There was a decline in NOD2 expression in about 67% of the cells transfected with NOD2-siRNAs compared with those transfected with an irrelevant-siRNA or the mock control. The second approach involved a polyphenol found in the plant *Curcuma longa*, commonly called curcumin, which is reported to inhibit NOD2 oligomerization and consequently NOD2 downstream signaling [28]. DENV2-infected and L18-MDP-transfected cells pre-treated with curcumin secreted significantly less IL-8 than the same groups without the curcumin pretreatment. Accordingly, IL-8 was quantified at ~756 pg/mL and 1390 pg/mL, respectively, in cells pretreated or not with curcumin and then stimulated with an L18-MDP transfection. Likewise, the level of IL-8 was measured at ~697 pg/mL and 1073 pg/mL, respectively, in cells pretreated or not with curcumin and then infected with DENV2 (Suppl. Fig. 4).

Gene silencing had a very similar effect. Secretion of IL-8 was determined to be at ~845 pg/mL and 1151 pg/mL, respectively, in cells transfected with NOD2-siRNAs or the irrelevant-siRNA, in both cases later stimulated with the transfection of L18-MDP. IL-8 production was at ~688 pg/mL and 983 pg/mL, respectively, in cells transfected with NOD2-siRNAs or the irrelevant-siRNA, in both cases later infected with DENV2. The basal level of IL-8 (in untreated cells) was ~480 pg/mL (Fig. 5A). NOD2 silencing also had a negative impact on IFN- α secretion. Cells transfected with NOD2-siRNAs or an irrelevant-siRNA and then treated with PIC showed levels at ~73 pg/mL and 133 pg/mL, respectively. The same two pretreatments followed by DENV2 infection resulted in levels of IFN- α at ~53 pg/mL and 110 pg/mL, respectively. IFN- α was not detected in untreated cells (Fig. 5B).

Figure 6



Φιγυρε 5. Γενε σιλενσινγ οφ NOΔ2 βψ σιPNAς δεσρεασεδ ζελλ σεσρετιον οφ ΙΛ-8 ανδ ΙΦN- α . THP-1 macrophage-like cells were gene-silenced with a mix of specific human NOD2-siRNAs or left intact with an irrelevant-siRNA. Subsequently, they were infected with DENV2 or transfected with L or PIC. Cell supernatants were then collected, and the cytokine levels were measured by ELISA. (A-B) The level of IL-8 was determined at 12 h and IFN- α at 24 h. Data in the bar graphs are expressed as the mean \pm SD from three independent assays. Significance was examined with the unpaired *t*-test and Mann-Whitney

U distribution: *** $p < 0.001$, ** $p < 0.05$, * $p < 0.05$, and ns: not significant. (C) Western blot on the silencing assay and levels of downregulation using NOD 2 specific siRNAs are shown.

NOD2 inhibition led to greater viral loads

An over 4-fold increase in viral load was produced in cells with NOD2 knocked down by treatment with specific siRNAs compared to cells with NOD2 unaffected by an irrelevant-siRNA (1.8×10^4 FFU/mL versus 4.4×10^3 FFU/mL, respectively). The same effect was observed in curcumin pretreated versus normal cells, in both cases later infected with DENV2. The level of viral titers rose more than 2.5-fold in the chemically treated versus normal cells (1.1×10^4 FFU/mL vs. 4.3×10^3 FFU/mL, respectively) (Fig. 6). The effect of the reduced expression or function of NOD2 on viral kinetics in infected cells (at 12, 24 and 48 hpi) was time-dependent beginning at 12 hpi, with the viral load increasing at 24 and again at 48 hpi. The level of titers at 24 hpi was $\sim 2.8\text{--}3.3 \times 10^3$ FFU/mL in untreated cells and those transfected with an irrelevant-siRNA, compared to $\sim 2.0 \times 10^4$ FFU/mL in the group transfected with NOD2-siRNAs. Similar data were found at 48 hpi, where titers were $\sim 1.1 \times 10^4$ FFU/mL in untreated cells and those transfected with an irrelevant-siRNA, compared to $\sim 2.6 \times 10^4$ FFU/mL in the group transfected with NOD2-siRNAs (Suppl. Fig. 5A).

Figure 7

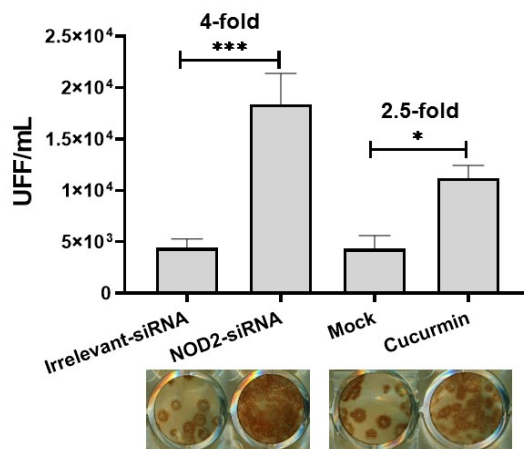


Figure 6. THP-1 macrophage-like cells with a reduced expression of NOD2 produced a higher level of viral titers. Cells were knocked down in NOD2 expression by using a mix of NOD2-siRNAs or inhibited in NOD2 signaling with the curcumin pretreatment. After NOD2 downregulation, the cells were infected with DENV2. At 24 hpi, supernatants were collected, and viral progeny from supernatants were quantified by a focus forming assay in C6/36 cells. (A) Viral titers are represented as focus forming units per milliliter (FFU/mL). Data in the bar graph are expressed as the mean \pm SD from three independent assays. Significance was determined with the unpaired *t*-test: * $p < 0.05$ and *** $p < 0.001$.

Discussion

PRRs are the first line of recognition for the defense against pathogens. During viral infections, two kinds of PRRs (TLRs and RLRs) are activated and potentiated. Additionally, members of the NLR family are vital for inflammatory functions during a viral infection. For example, NLRP3 [15-16] and NLRX1 regulate functions of the RIG-I/MAVS pathway [30] and NOD2 [19-22], a less studied effector, is also important in

viral infections.

In monocytes, macrophages and dendritic cells, the immediate response at early stages of a DENV2 infection is rapid and coordinated, mediated by TLR3, TLR7, TLR8, RIG-I and NLRP3 [10,13-15]. Additionally, the activation of other intracellular sensors located in the cytosol contributes to the establishment of this response. One very dynamic molecule is NOD2, which interacts with several effectors that participate in either proinflammatory or antiviral activity.

According to the current experimental results, NOD2 mRNA and protein expression was enhanced in THP-1 macrophage-like cells in response to an *in vitro* DENV-2 infection. Singular patterns of subcellular distribution of NOD2 expression was observed in the cells following treatment with a NOD2 agonist (L18-MDP) or infection with DENV2, suggesting that NOD2 may be present in defined vesicles (e.g., endosomes), as previously reported [31]. However, further research is necessary to identify the nature of the vesicles. The expression of NOD2 in the cells was also induced by a PIC, measured at 12. Therefore, a positive regulation of NOD2 appears to be mediated by these molecules, as has been documented for PIC [20].

Interestingly, the expression of elevated levels of NOD2 was exhibited in DENV-2-infected cells but not the untreated cells, which was confirmed by the detection of viral NS3. Thus, active DENV2 replication seems to be necessary to stimulate the up-regulation of NOD2. Although the latter molecule has been significantly associated only with homeostatic regulation in intestinal epithelial cells [32], its involvement in key processes of the proinflammatory and antiviral immune response is clear [33]. Consequently, the current study aimed to investigate the participation of NOD2 in the immune response to a DENV2 infection in an experimental model of THP-1 macrophage-like cells. Macrophages represent one of the main targets of the dengue virus and have a pivotal role in the immune response to a dengue infection. During infection with various RNA viruses, according to previous reports, NOD2 is activated and triggers a protective innate immune response against pathogens, mediated by interactions with adaptors such as RIP2, MAVS, OAS2 and CARD9 [34].

The protein interactions between NOD2 and numerous effectors might be significant for the course and effect of the immune response [35]. Of all NOD2-related effectors described in the literature, only those with a substantial antiviral activity were herein evaluated, being RIP2, and MAVS. Co-localization sites were determined at several post-treatment time points for NOD2-RIP2, and NOD2-MAVS in DENV2-infected and agonist-stimulated cells. Co-location was more evident for NOD2-RIP2 and NOD2-MAVS.

To provide greater insights into these discoveries, the aforementioned interactions were analyzed by co-immunoprecipitation assays. NOD2 was found to interact with RIP2, and MAVS in infected cells as well as in agonist-stimulated cells, and at distinct times post-stimuli. Hence, NOD2 is a dynamic molecule with different functions in the current infection model, mainly during the early response against DENV2. Considering the previous information, we propose that the NOD2-RIP2 interaction led to the generation of inflammatory cytokines and the NOD2-MAVS interaction to a type I IFN response, which has been described for a variety of RNA viruses. Further research is needed on the overall mechanisms involved.

The present findings after knocking down NOD2 expression or signaling contribute to a more in-depth understanding of the overall effect of this molecule on cell function during a dengue infection. NOD2 downregulation by specific siRNAs (versus cells with normal NOD2) correlated with a reduced secretion of IL-8 and IFN- α in DENV2-infected cells. Inhibition of NOD2 signaling by pretreating THP-1 cells with curcumin (versus cells with normal NOD2) afforded a similar decline in the expression of these cytokines in DENV2-infected cells. However, only early time points were examined the possibility that DENV counteracts some antiviral molecules later in the infection must be further examined.

Subsequently, an evaluation was made as to whether NOD2 misfunction in the cells infected with DENV2 had an impact on viral loads. A higher level of viral titers was detected in cells with a decreased expression or signalization of NOD2, and the load increased with the passage of post-infection time. Overall, the results demonstrate a formerly unknown role for NOD2 during DENV2 infection of THP-1 macrophage-like cells: limiting the production of new viral progeny. This is a very significant finding since it indicates that NOD2 either potentiates or initiates the antiviral response to combat viral replication, a trait found for this protein

in other viral infections. For instance, the foot-and-mouth disease virus counteracts NOD2 to antagonize antiviral activity [36].

NOD-2 activation has been a striking finding arose during SARS-CoV2 pandemic research, documenting a Nodosome activation (NOD2-RIP2) during Zika virus, DENV and SARS-CoV2 infection in cell lines [37].

In conclusion, the NOD2 receptor was herein upregulated and activated at the early stage of a DENV2 infection, concomitantly with active viral replication in macrophages derived from the THP-1 cell line. The activation of NOD2 during the infection led to its interaction with RIP2 and MAVS (measured at several post-infection times), and elicited the secretion of IL-8 and IFN- α . Through these mechanisms, NOD2 was involved in limiting the replication of new DENV2 viral particles in THP-1 macrophage-like cells.

Acknowledgments: The authors are very grateful to our sponsors: Jorge Ortega-Reyes for providing the anti-rabbit-IgG-APC, Antonina Oltra-Ramírez for the anti-human NOD2, and Alejandro Ayala-Castro for the IL-8 and IFN- α ELISA kits. We are deeply appreciative of Dr. Eneida Campos-Guzmán for all her assistance in the confocal microscopy studies, and of Inci Enid Ramírez-Bello (a student at the *Posgrado en Inmunología*) for all her help. L.-A.G., G.-P.B.E. and S.M.I. are COFAA and EDI fellows. This investigation was supported by the Secretaría de Investigación y Posgrado (SIP-IPN). Alan Larsen for critically reading and editing our manuscript.

Conflicts of Interest: The authors have no conflicts of interest to declare.

Funding: This research project was supported by grants to S.M.I. (SIP20151797 and SIP20161585) from the SIP-IPN, and the fellowship to D.-M.D.A. (356583) from the Consejo Nacional de Ciencia y Tecnología.

Author Contributions: Conceptualization, D.-M.D.A. and S.M.I; methodology, D.-M.D.A. and N.-A.D.; validation, N.-A.D., G.-P.B.E., L.-A.G. and S.M.I; formal analysis, D.-M.D.A., G.-P.B.E. and S.M.I; investigation, D.-M.D.A. and S.M.I; resources, G.-P.B.E., L.-A.G. and S.M.I; data curation, M.I.S.; writing of the original draft, D.-M.D.A. and S.M.I; writing, review & editing, D.-M.D.A., N.-A.D., G.-P.B.E., C.-C.J. and S.M.I; funding acquisition, S.M.I. and D.-M.D.A. All authors read and approved the final version of the manuscript.

References

1. Bhatt, S.; Gething, P.W.; Brady, O.; Messina, J.P.; Farlow, A.W.; Moyes, C.L.; Drake, J.M.; Brownstein, J.S.; Hoen, A.G.; Sankoh, O.; Myers, M.F.; George, D.B.; Jaenisch, T.; Wint, G.R.; Simmons, C.P.; Scott, T.W.; Farrar, J.J.; Hay, S.I. The global distribution and burden of dengue. *Nature*. 2013;496(7446):504-507.
2. Rico-Hesse, R. Dengue virus virulence and transmission determinants. *Curr Top Microbiol Immunol*. 2010;338:45-55.
3. Mukhopadhyay, S.; Kuhn, R.J.; Rossmann, M.G. A structural perspective of the flavivirus life cycle. *Nat Rev Microbiol*. 2005;3(1):13-22.
4. Wu, S.J.; Grouard-Vogel, G.; Sun, W.; Mascola, J.R.; Brachtel, E.; Putvatana, R.; Louder, M.K.; Filgueira, L.; Marovich, M.A.; Wong, H.K; Blauvelt, A.; Murphy, G.S.; Robb, M.L.; Innes, B.L.; Birx, D.L.; Hayes, C.J.; Frankel, S.S. Human skin Langerhans cells are targets of dengue virus infection. *Nat Med*. 2000;6(7):816-820.
5. Marovich, M.; Grouard-Vogel, G.; Louder, M.; Eller, M.; Sun, W.; Wu S.J.; Putvatana, R.; Murphy, G.; Tassaneetrithep, B.; Burgess, T.; Birx, D.; Hayes, C.; Schlesinger-Frankel, S.; Mascola, J. *J Invest Dermatol Symp Proc*. 2001;6(3):219-224.
6. Jessie, K.; Fong, M.Y.; Devi, S.; Lam, S.K.; Wong, K.T. Localization of dengue virus in naturally infected human tissues, by immunohistochemistry and in situ hybridization. *J Infect Dis*. 2004;189(8):1411-1418.
7. Kwan W.H.; Navarro-Sanchez, E.; Dumortier, H.; Decossas, M.; Vachon, H.; dos Santos, F.B.; Fridman, H.W.; Rey F.A.; Harris, E.; Despres, P.; Mueller C.G. Dermal-type macrophages expressing CD209/DC-SIGN show inherent resistance to dengue virus growth. *PLoS Negl Trop Dis* .

- 2008;2(10):e311. Published 2008 Oct 1.
8. Takaoka, A.; Yanai, H. Interferon signalling network in innate defence. *Cell Microbiol.* 2006;8(6):907-922.
 9. McNab, F.; Mayer-Barber, K.; Sher, A.; Wack, A.; O'Garra, A. Type I interferons in infectious disease. *Nat Rev Immunol* . 2015;15(2):87-103.
 10. Wang, J.P.; Liu, P.; Latz, E.; Golenbock, D.T.; Finberg, R.W.; Libraty, D.H. Flavivirus activation of plasmacytoid dendritic cells delineates key elements of TLR7 signaling beyond endosomal recognition. *J Immunol* . 2006;177(10):7114-7121.
 11. Chang, T.H.; Liao, C.L.; Lin, Y.L. Flavivirus induces interferon-beta gene expression through a pathway involving RIG-I-dependent IRF-3 and PI3K-dependent NF-kappaB activation. *Microbes Infect.*2006;8(1):157-171.
 12. Loo, Y.M.; Fornek, J.; Crochet, N.; Bajwa, G.; Perwitasari, O.; Martinez-Sobrido, L.; Akira, S.; Gill, M.A.; García-Sastre, A.; Katze, M.G.; Gale Jr, M. Distinct RIG-I and MDA5 signaling by RNA viruses in innate immunity. *J Virol.* 2008;82(1):335-345.
 13. Tsai, Y.T.; Chang, S.Y.; Lee, C.N.; Kao, C.L. Human TLR3 recognizes dengue virus and modulates viral replication in vitro. *Cell Microbiol* . 2009;11(4):604-615.
 14. Nasirudeen, A.M.; Wong, H.H.; Thien, P.; Xu, S.; Lam, K.P.; Liu, D.X. RIG-I, MDA5 and TLR3 synergistically play an important role in restriction of dengue virus infection. *PLoS Negl Trop Dis* . 2011;5(1):e926.
 15. Wu, M.F.; Chen, S.T.; Yang, A.H.; Lin, W.W.; Lin, Y.L.; Chen, N.J.; Tsai, I.S.; Li, L.; Hsieh, S.L. CLEC5A is critical for dengue virus-induced inflammasome activation in human macrophages. *Blood* . 2013;121(1):95-106.
 16. Hottz, E.D.; Lopes, J.F.; Freitas C.; Valls-de-Souza, R.; Oliveira, M.F.; Bozza, M.T.; Da Poian, A.T.; Weyrich, A.S.; Zimmerman, G.A.; Bozza, F.A.; Bozza, P.T. Platelets mediate increased endothelium permeability in dengue through NLRP3-inflammasome activation. *Blood* . 2013;122(20):3405-3414.
 17. Inohara, N.; Nuñez, G. NODs: intracellular proteins involved in inflammation and apoptosis. *Nat Rev Immunol* . 2003;3(5):371-382.
 18. Moreira, L.O.; Zamboni, D.S. NOD1 and NOD2 Signaling in Infection and Inflammation. *Front Immunol* . 2012;3:328.
 19. Tominaga, K.; Dube, P.H.; Xiang, Y.; Bose, S. Activation of innate immune antiviral responses by Nod2. *Nat Immunol* . 2009;10(10):1073-1080.
 20. Kim, Y.G.; Park, J.H.; Reimer, T.; Baker, D.P.; Kawai, T.; Kumar, H.; Akira, S.; Wobus, C.; Nuñez G. Viral infection augments Nod1/2 signaling to potentiate lethality associated with secondary bacterial infections. *Cell Host Microbe* . 2011;9(6):496-507.
 21. Lupfer, C.; Thomas, P.G.; Anand, P.K.; Vogel, P.; Milasta, S.; Martinez, J.; Huang, G.; Green, M.; Kundu, M.; Chi, H.; Xavier, R.J.; Green, D.R.; Lamkanfi, M.; Dinarello, C.A.; Doherty, P.C.; Kanneganti, T.D. Receptor interacting protein kinase 2-mediated mitophagy regulates inflammasome activation during virus infection. *Nat Immunol* . 2013;14(5):480-488
 22. Dugan, J.W.; Albor, A.; David, L.; Fowlkes, J.; Blackledge, M.T.; Martin, T.M.; Planck, S.R.; Rosenzweig, H.L.; Rosenbaum, J.T.; Davey, M.P. Nucleotide oligomerization domain-2 interacts with 2'-5'-oligoadenylate synthetase type 2 and enhances RNase-L function in THP-1 cells. *Mol Immunol* . 2009;47(2-3):560-566.
 23. Duran, A.; Valero, N.; Mosquera, J.; Fuenmayor, E.; Alvarez-Mon, M. Gefitinib and pyrrolidine dithiocarbamate decrease viral replication and cytokine production in dengue virus infected human monocyte cultures. *Life Sci* . 2017;191:180-185.
 24. Morchang, A.; Yasamut, U.; Netsawang, J.; Noisakran S.; Wongwiwat, W.; Songprakhon, P.; Srisawat, C.; Puttikhunt, C.; Kasinrerak W.; Malasit, P.; Yenchitsomanus, P.T.; Limjindaporn, T. Cell death gene expression profile: role of RIPK2 in dengue virus-mediated apoptosis. *Virus Res* . 2011;156(1-2):25-34.
 25. Olganier, D.; Scholte, F.E.; Chiang, C.; Albuлесcu, I.C.; Nichols, C.; He, Z.; Lin, R.; Snijder, E.J.; van Hemert, M.J.; Hiscott, J. Inhibition of dengue and chikungunya virus infections by RIG-I-mediated type I interferon-independent stimulation of the innate antiviral response. *J Virol* . 2014;88(8):4180-4194.

26. Lin, R.J.; Yu, H.P.; Chang, B.L.; Tang, W.C.; Liao, C.L.; Lin, Y.L. Distinct antiviral roles for human 2',5'-oligoadenylate synthetase family members against dengue virus infection. *J Immunol* . 2009;183(12):8035-8043.
27. Jadhav, N.J.; Gokhale, S.; Seervi, M.; Patil, P.S.; Alagarasu, K. Immunomodulatory effect of 1, 25 dihydroxy vitamin D₃ on the expression of RNA sensing pattern recognition receptor genes and cytokine response in dengue virus infected U937-DC-SIGN cells and THP-1 macrophages. *Int Immunopharmacol* . 2018;62:237-243.
28. Huang, S.; Zhao, L.; Kim, K.; Lee, D.S.; Hwang, D.H. Inhibition of Nod2 signaling and target gene expression by curcumin. *Mol Pharmacol* . 2008;74(1):274-281.
29. Castañeda-Sánchez, J.I.; Domínguez-Martínez, D.A.; Olivares-Espinosa, N.; García-Pérez, B.E.; Loroño-Pino, M.A.; Luna-Herrera, J.; Salazar, M.I. Expression of Antimicrobial Peptides in Human Monocytic Cells and Neutrophils in Response to Dengue Virus Type 2. *Intervirology* . 2016;59(1):8-19.
30. Allen, I.C.; Moore, C.B.; Schneider, M.; Lei, Y.; Davis, B.K.; Scull, M.A.; Gris, D.; Roney, K.E.; Zimmermann, A.G.; Bowzard, J.B.; Ranjan, P.; Monroe, K.M.; Pickles, R.J.; Sambhara, S.; Ting J.P. NLRX1 protein attenuates inflammatory responses to infection by interfering with the RIG-I-MAVS and TRAF6-NF- κ B signaling pathways. *Immunity* . 2011;34(6):854-865.
31. Nakamura, N.; Lill, J.R.; Phung, Q.; Jiang, Z.; Bakalarski, C.; de Mazière, A.; Klumperman, J.; Schlatter, M.; Delamarre, L.; Mellman, I. Endosomes are specialized platforms for bacterial sensing and NOD2 signalling. *Nature* . 2014;509(7499):240-244.
32. Ferrant, A.; Al-Nabhani, Z.; Solà-Tapias, N.; Mas, E.; Hugot, J-P.; Barreau, F. NOD2 expression in intestinal epithelial cells protects toward the development of inflammation and associated carcinogenesis. *Cell Mol Gastro Hepat* 2019; 7(2): 357-369.
33. Negroni, A.; Pierdomenico, M.; Cucchiara, S.; Stronati, S. NOD2 and inflammation. *J Inflamm Res* 2018; 11:49-60.
34. Domínguez-Martínez, D.A.; Núñez-Avellaneda, D.; Castañón-Sánchez, C.A.; Salazar, M.I. NOD2: Activation during bacterial and viral infections, polymorphisms and potential as therapeutic target. *Rev Invest Clin* 2018; 70(1):18-28.
35. Bottermann, M.; James, L.C. Intracellular antiviral immunity. *Adv Virus Res* 2018; 1001: 309-354.
36. Liu, H.; Zhu, Z.; Xue, Q.; Yang, F.; Cao, W.; Zhang, K.; Liu, X.; Zheng, H. Foot-and-Mouth disease virus antagonizes NOD2-mediated antiviral effects by inhibiting NOD2 protein expression. *J Virol* 2019; 93(11):e00124-19.
37. Limonta, D.; Dyna-Dagman, L; Branton, W; Makio, T; Wozniak, R; Power, C; Hobman T. Nodosome inhibition as a novel broad-spectrum antiviral strategy against arboviruses and SARS-CoV-2. bioRxiv 2020.11.05.370767; doi: <https://doi.org/10.1101/2020.11.05.370767>